Remote Sensing of Inland Waters: Background and Current State-of-the-Art

Chapter · May 2017

DOI: 10.1016/B978-0-12-804644-9.00001-X

3 authors:

Igor Ogashawara
Leibniz-Institute of Freshwater Ecology and Inland Fish…

Deepak R Mishra
University of Georgia

Anatoly Gitelson
Technion - Israel Institute of Technology

Chapter 1

Remote Sensing of Inland Waters: Background and Current State-of-the-Art

Igor Ogashawara[1], Deepak R. Mishra[2], and Anatoly A. Gitelson[3,4]
[1]Indiana University—Purdue University at Indianapolis (IUPUI), Indianapolis, IN, United States, [2]University of Georgia (UGA), Athens, GA, United States, [3]Israel Institute of Technology, Haifa, Israel, [4]University of Nebraska-Lincoln (UNL), Lincoln, NE, United States

1.1 INLAND WATERS

This book is designed to highlight the theories, past developments, and current state-of-the-art knowledge in bio-optical modeling of inland waters. This area of remote sensing research has been intensively developed in the last 30 years primarily using the concepts and theories from optical oceanography. The focus of this book is squarely placed on inland waters because of the lack of a coherent and comprehensive synthesis of multidecadal bio-optical research on this important environment. Inland waters are aquatic environments typically confined within the land boundaries and provide exceptionally important ecological, environmental, hydrological, and socioeconomic services to mankind and the environment. The Millennium Ecosystem Assessment, a taskforce initiated by United Nations Secretary-General in 2001, generated a list of services provided by or derived from inland waters which were divided into four categories: provisioning (i.e., food supply, water supply, and biodiversity); regulating (i.e., climate regulation, hydrological flows, and pollution control); cultural (i.e., recreational, aesthetic, and educational); and supporting (i.e., soil formation, nutrient cycling, and pollination) (Millennium Ecosystem Assessment MEA, 2005).

The term "inland waters" is used wherever possible unless a specific ecosystem type is mentioned, such as lakes, reservoirs, rivers, ponds, swamps, wetlands, and even coastal areas. Inland waters represent an extremely diverse environment including a broad array of shapes and sizes, and physical, chemical, and optical properties. For example, inland waters

Bio-optical Modeling and Remote Sensing of Inland Waters.
DOI: http://dx.doi.org/10.1016/B978-0-12-804644-9.00001-X

could be fresh (Caspian Sea, western Asia-eastern Europe; Great Lakes, USA), saline (Dead Sea, Middle East), or brackish (Lake Pontchartrain, USA; Lake Chilika, India). The extent and distribution of inland waters is poorly and unevenly known at the global scale, since their size varies from small (i.e., ponds) to very large (i.e., Great Lakes) often creating inconsistencies in detection and inventory over broad geographic scale. Verpoorter et al. (2014) used GeoCover product developed using imageries from Enhanced Thematic Mapper Plus (ETM^+) onboard Landsat-7 satellite to map all inland water bodies greater than $0.002\,km^2$. Their findings contained geographic and morphometric information for approximately 117 million inland aquatic systems with a combined surface area of approximately $5 \times 10^6\,km^2$. Although inland waters only comprise a small percentage of Earth's total land surface, they play an essential role in biogeochemical cycle and are very important in the history of mankind (Bastviken et al., 2011).

Inland water bodies serve as sentinels to changing environment, such as climate change, developmental pressure, and land use land cover change. Rapid and uncontrolled environmental change, such as deforestation and reduction of vegetation cover, nutrient pollution, drought, urbanization, and engineered modifications to watershed most often result in negative impact including accelerated eutrophication, proliferation of toxic blue-green algae, extreme turbidity and deterioration of water clarity, loss of aquatic benthos, and harmful effect on human and animal health. Considering the vital uses of inland waters, water quality management needs to be a top priority for environmental regulatory agencies around the world. The National Research Council (NRC) published a comprehensive report entitled "The Drama of the Commons" highlighting seven key challenges in environmental resource management (National Research Council NRC, 2002). Included among those were "low-cost enforcement of rules" and "monitoring the resource and users' compliance with rules," which highlighted the need for a low-cost environmental monitoring program using remote sensing technologies. Rapid monitoring surveys using remote sensing should be conducted frequently along with less frequent field-based methods as an effective water quality management strategy (Ostrom et al., 2003). As opposed to the traditional field-based methods to monitor water quality, which are usually costly and labor intensive, remote sensing offers a low-cost, high frequency, broad coverage, and practical alternative for water quality assessment and monitoring (Duan et al., 2010; Hadjimitsis and Clayton, 2009). The main advantage of remote sensing is its capability to perform frequent large-scale synoptic monitoring of water resources and, therefore, the development of new techniques or fine-tuning of existing bio-optical models (a.k.a. bio-optical algorithms), and methods for using remote sensor derived products are essential for accurate monitoring inland water resources and isolating the natural and anthropogenic stressors.

1.2 REMOTE SENSING OF INLAND WATERS

The utilization of remote sensing techniques to monitor aquatic environments was initiated during 1960s by analyzing ocean color under the assumption that chlorophyll-*a* (chl-*a*), a proxy for phytoplankton biomass, and surface temperature could be estimated remotely (Morel and Gordon, 1980; Gordon et al., 1988). Based on these assumptions, oceanographers started to remotely monitor the optical properties of water constituents, such as phytoplankton, colored dissolved organic matter (CDOM) and total suspended solids (TSS) (Jerlov, 1968; Preisendorfer, 1976; Morel, 2001). As a result, the concepts of hydrologic optics and radiative transfer theory were developed and formed the basis of what is currently known as bio-optical modeling. However, the application of these theories and concepts developed by oceanographers were applied to inland waters only during the last three decades concomitant to the extensive use of bio-optical models to monitor optically active water constituents, such as chl-*a*, TSS, and CDOM (Jerlov, 1968, 1976; Gordon and Morel, 1983; Morel, 2001).

Nevertheless, application of remote sensing techniques to inland waters can be quite different from open ocean waters mainly because of the variable composition of water constituents. Morel and Prieur (1977) proposed a two-tier classification of water bodies: Case 1 and Case 2. This classification was based on the reflectance ratio at 443 and 550 nm. The ratio should be greater than 1.0 for Case 1 and less than 1.0 for Case 2 waters. Gordon and Morel (1983) proposed new definitions for Case 1 and Case 2 waters. They classified Case 1 waters as waters whose optical properties are determined mainly by phytoplankton and the other covarying compounds, such as CDOM and detritus. Case 2 waters are waters whose optical properties are significantly influenced by other constituents, such as mineral particles and CDOM, and their concentrations do not covary with phytoplankton. However, this classification showed several problems, such as the misinterpretation that inland waters mostly belong to Case 2 category, when it is possible that these water bodies can be dominated by phytoplankton or its derivatives, which would make them Case 1 (Mobley et al., 2004). Despite of the criticisms about the classification, it was used widely by researchers to categories water types for a quick overview.

Because of the presence of multiple constituents at different composition [i.e., phytoplankton, nonalgal particles (NAP), CDOM, and detritus], the use of remote sensing for monitoring inland water quality has been far less successful compared to open oceans. The complex interaction among the water constituents, which is often intensified by anthropogenic actions, creates uncertainty in remote sensing models designed for inland waters. Within the same inland aquatic system, it is possible to have different regions dominated by different constituents. For example, Gurlin et al. (2011) showed that for different sampling locations in Fremont Lakes, USA, the absorption

coefficients of water constituents, phytoplankton [$a_{phy}(\lambda)$], nonalgal particles [$a_{NAP}(\lambda)$], and CDOM [$a_{CDOM}(\lambda)$], varied considerably along with constituents concentrations (Fig. 1.1). In the blue region, the contribution of absorption coefficient of water [$a_w(\lambda)$] is minimal while the major contributors are $a_{CDOM}(\lambda)$ and $a_{NAP}(\lambda)$. $a_{phy}(\lambda)$ contribution in the blue region is mostly minor and varied based on the chl-*a* concentration. In the green region, the absorption coefficients of $a_{CDOM}(\lambda)$, $a_{NAP}(\lambda)$, and $a_{phy}(\lambda)$ are smaller than in the blue and $a_w(\lambda)$ is higher. Ocean color algorithms (e.g., OC4v4) that use blue and green spectral channels often provide a relatively accurate estimate of chl-*a* in ocean waters (Case 1) where the total nonwater absorption is dominated by phytoplankton. However, inland waters, which are optically complex, spectral channels in the blue-green region, are heavily affected by an intricate interaction between a variety of water constituents, such as phytoplankton, CDOM, detritus, and tripton, and cannot be used to resolve any constituent. Only in the red spectral region, beyond 650 nm, absorption is

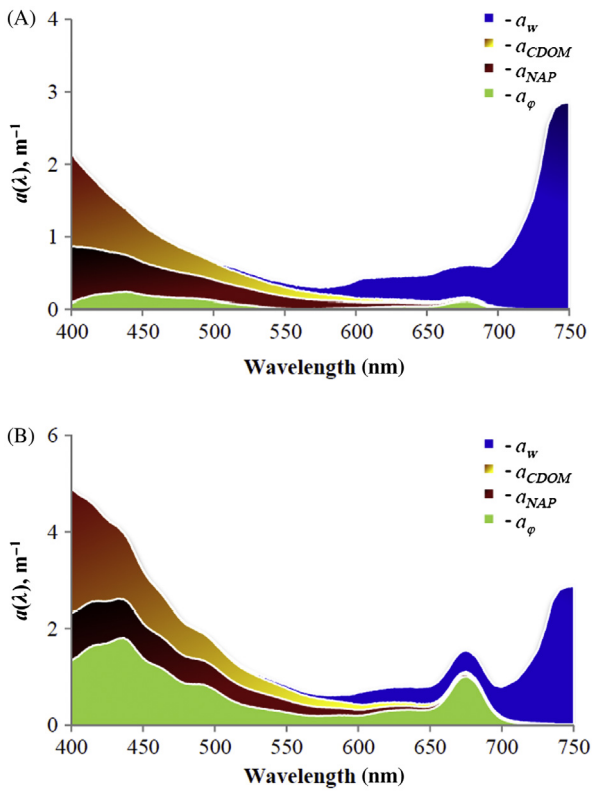

FIGURE 1.1 Absorption coefficients of phytoplankton, nonorganic particles, dissolved organic matter, and pure water, $a_{phy}(\lambda)$, $a_{NAP}(\lambda)$, $a_{CDOM}(\lambda)$, and $a_w(\lambda)$, for two sampling stations with chl-*a* concentrations of 4.6 mg m^{-3} (A) and 58.1 mg m^{-3} (B) ($a_{phy}(\lambda)$ is the same as a_φ in the figure). *Source: Figure 4.1 from Gurlin (2012).*

mainly governed by phytoplankton and pure water; therefore, red-near infrared (NIR) wavelengths have been found to be more appropriate for the development of bio-optical models for inland waters, particularly in waters where chl-*a* concentration is above 10 μg/L (Gitelson, 1992; Mishra and Mishra, 2012).

Because of these complexities due to mixed constituents, commonly found in inland waters, this book is aimed at synthesizing the current state-of-the-art in terms of both knowledge and applications to monitor these aquatic environments.

1.3 FUNDAMENTAL BIO-OPTICAL PROPERTIES

Remote sensing of inland waters is based on the optical properties of water constituents (e.g., Morel, 2001). These properties can be divided into two categories: (1) properties that depend on the medium and the directional structure of the ambient light field, known as apparent optical properties (*AOPs*), and (2) those which depend only on the medium and are independent of the ambient light field, known as inherent optical properties (*IOPs*) (Preisendorfer, 1976). Optical properties, such as irradiance reflectance (R), above and below water remote sensing reflectance (R_{rs} or r_{rs} respectively), and various diffuse attenuation functions (K) are *AOPs*, since they vary according to the composition of the medium and the light field. Properties, such as absorption (a) and scattering (b) coefficients, which vary based on just the composition of the medium or constituents, are *IOPs*. A more detailed description about AOPs and IOPs is provided in Chapter 2 which covers physical principles and radiative transfer theory applied to inland waters.

For remote sensing of inland waters, the most commonly used *AOP* is R_{rs}. R_{rs} is defined as the ratio of water-leaving radiance (L_w) to downwelling irradiance (E_d), expressed in terms of *per steradian* (sr^{-1}). In case of IOPs, absorption properties of water constituents are the most commonly used parameters since instruments for measuring scattering in inland waters are not widely deployed and more research is needed to evaluate their performance in these optically complex waters.

To understand the optical properties of a medium (e.g., water column), one needs to recognize the Kubelka–Munk remission function. The function explains the infinite reflectance (R_∞) of an ideal layer of turbid media in which a further increase in thickness results in no noticeable difference in reflectance (Kubelka and Munk, 1931). R_∞ is proportional to the ratio of the absorption coefficient to the scattering coefficient of the media (Kubelka and Munk, 1931; Kortum, 1969). Studies have shown that the Kubelka–Munk remission function relates very closely (determination coefficient above 0.99) to the inverse reflectance of leaves (Gitelson et al., 2003) and water (Dall'Olmo et al, 2003). Thus, inverse reflectance may be used as proxy of absorption by phytoplankton pigments, NAP, CDOM, and water. Fig. 1.2

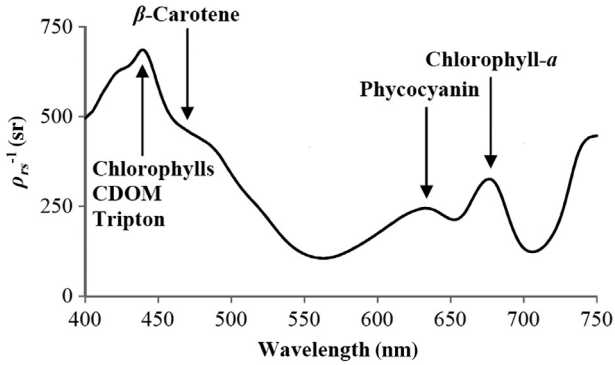

FIGURE 1.2 Typical inland waters inverse R_{rs} spectrum. The positions of the absorption peaks by constituents, such as chl-*a*, PC, NAP, and CDOM are labeled. *Source: Figure 3.16 from Gurlin (2012).*

shows distinctive spectral features of an inverse R_{rs} spectrum acquired from an inland water body, which has a high absorption in the blue spectral region due to the combined absorption by phytoplankton pigments, β-Carotene, NAP, and CDOM. The absorption peak around 625 nm is related to the presence of phycocyanin (PC), a proxy for cyanobacteria, and another absorption peak around 675 nm is related to the absorption by chl-*a*. These complex interactions between the constituents and their corresponding spectral features form the foundation for the development of bio-optical models for inland waters.

A list of research studies reporting absorption coefficients, such as a_{CDOM}, a_{NAP}, and a_{phy} from different inland waters is provided in Table 1.1. It is possible to further partition some of the primary absorption coefficients using decomposition algorithms. For example, a_{phy} can be decomposed into absorption coefficients of chl-*a* ($a_{chl\text{-}a}$) and *PC* (a_{PC}) (Simis et al., 2005, Mishra et al., 2013, 2014); and a_{NAP} can be partitioned into absorption coefficients of minerogenic particles (a_m) and organic detritus (a_d) (Peng and Effler, 2013).

IOPs vary not only across geographic regions but also within the same site (Table 1.1). For example, Gons et al. (2008) reported a_{CDOM} ranges from Finger Lakes, New York which varied from 0.06 to 67 m^{-1}. In addition, studies such as Matthews and Bernard (2013), which analyzed the three absorption coefficients in multiple lakes, demonstrated the complexities of interaction between constituents and their optical properties in inland waters. The complexity is mainly due to the spatial-temporal variability of the water constituents at the same site. In other words, the dominant constituent in the water column at a study site may not only change spatially across short distances but also across seasons and even daily (Yacobi et al., 1995; Huang et al., 2015). Multiple dominant constituents over relatively short period of

TABLE 1.1 List of Studies Reporting Absorption Coefficients of Optically Active Constituents Measured at Various Inland Water Bodies

Reference	Site	Location	Wavelength (nm)	Absorption Coefficient (m^{-1})
		a_{CDOM}		
Dall'Olmo and Gitelson (2005)	Eastern Nebraska water bodies	Nebraska, USA	440	0.5–4.4
Dekker (1993)	Vecht Lakes	The Netherlands	440	1.19–3.74[a]
Gitelson et al. (2008)	Nebraska Lakes (2005)	Nebraska, USA	440	0.3–1.77
Gons et al. (2008)	Finger Lakes	New York, USA	440	0.06–67
Gurlin et al. (2011)	Fremont Lakes (2008)	Nebraska, USA	440	0.46–1.46
Gurlin et al. (2011)	Fremont Lakes (2009)	Nebraska, USA	440	0.35–1.35
Kutser et al. (2005a)	Finnish Lakes	Southern Finland	420	1.28–7.74
Kutser et al. (2015)	Lake Mälaren	Stockholm, Sweden	443	2.7–4.0
Le et al. (2009)	Lake Tai	China	440	0.02–1.42
Matthews and Bernard (2013)	Lake Hartbeespoort	South Africa	442	0.63–4.13[b]
Matthews and Bernard (2013)	Lake Loskop	South Africa	442	0.75–1.87[b]
Matthews and Bernard (2013)	Lake Theewaterskloof	South Africa	442	1.22–2.49[b]
Mishra et al. (2014)	Catfish Ponds	Mississippi, USA	443	3.2–4.33[c]
Song et al. (2014)	Central Indiana Reservoirs	Indiana, USA	440	0.58–3.23
		a_{NAP}		
Dall'Olmo and Gitelson (2005)	Eastern Nebraska water bodies	Nebraska, USA	440	0.4–6.7[d]
Gitelson et al. (2008)	Nebraska Lakes (2005)	Nebraska, USA	440	0.13–4.34[d]
Gurlin et al. (2011)	Fremont Lakes (2008)	Nebraska, USA	675	0.003–0.294

(*Continued*)

TABLE 1.1 (Continued)

Reference	Site	Location	Wavelength (nm)	Absorption Coefficient (m^{-1})
Gurlin et al. (2011)	Fremont Lakes (2009)	Nebraska, USA	675	0.007–0.113
Le et al. (2009)	Lake Tai	China	440	0.57–7.16
Matthews and Bernard (2013)	Lake Hartbeespoort	South Africa	442	0.07–1.74[d]
Matthews and Bernard (2013)	Lake Loskop	South Africa	442	0.1–1.57[d]
Matthews and Bernard (2013)	Lake Theewaterskloof	South Africa	442	0.51–2.26[d]
		a_{phy}		
Dall'Olmo and Gitelson (2005)	Eastern Nebraska water bodies	Nebraska, USA	678	1.0–6.0
Gurlin et al. (2011)	Fremont Lakes (2008)	Nebraska, USA	675	0.04–4.45
Gurlin et al. (2011)	Fremont Lakes (2009)	Nebraska, USA	675	0.04–2.72
Le et al. (2009)	Lake Tai	China	675	0.06–3.99
Li et al. (2013)	Central Indiana Reservoirs	Indiana, USA	665	0.439–3.87[e]
Li et al. (2013)	Central Indiana Reservoirs	Indiana, USA	665	0.037–2.51[e]
Matthews and Bernard (2013)	Lake Hartbeespoort	South Africa	442	1.73–455.32
Matthews and Bernard (2013)	Lake Loskop	South Africa	442	0.05–11.12
Matthews and Bernard (2013)	Lake Theewaterskloof	South Africa	442	0.41–2.43
Mishra et al. (2014)	Catfish Ponds 1	Mississippi, USA	443	10.27–15.55
Mishra et al. (2014)	Catfish Ponds 1	Mississippi, USA	665	3.96–6.23

[a]*Reported as aquatic humus absorption coefficient.*
[b]*Reported as gelbstoff absorption coefficient.*
[c]*Reported as colored detrital matter absorption coefficient.*
[d]*Reported as detrital absorption coefficient.*
[e]*Reported as total less water absorption coefficient* ($a_{t\text{-}w}$).

time seen in inland water environments is not common for open ocean environments which makes the remote sensing of inland waters a challenging task. It can also be seen from Table 1.1, studies quantifying absorption coefficients of constituents in inland waters are fairly recent indicating that the development of robust models for the estimations of IOPs in inland waters is a relatively new field of research.

The variability in the composition of constituents and the associated IOPs within an aquatic system can affect the magnitude and shape of R_{rs}. To exemplify this, data from three water bodies with different trophic status are used: two tropical hydroelectric reservoirs (Itumbiara and Funil Reservoirs) in Brazil and catfish ponds in Mississippi, USA. The Itumbiara Hydroelectric Reservoir located in Central Brazil is an oligotrophic reservoir. Funil Hydroelectric Reservoir is a mesotrophic reservoir located in Southeast Brazil. The catfish ponds located at Delta Research Extension Center near Stoneville, MS, USA are hypereutrophic in nature.

Fig. 1.3 shows the average R_{rs} spectra normalized at 575 nm for the three study sites. The normalization to a specific wavelength is usually performed to allow the intercomparison of R_{rs} spectra from different water bodies. The R_{rs} spectrum for the oligotrophic Itumbiara reservoir showed a very distinct

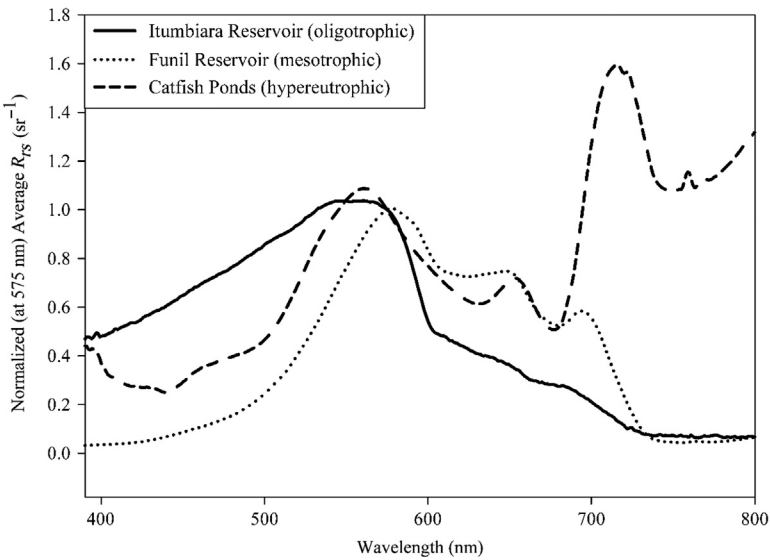

FIGURE 1.3 Average normalized R_{rs} for three inland water bodies representing oligotrophic waters (Itumbiara Reservoir, chl-*a*: 0.25–10.20 μg/L; TSS: 0.25–1.81 mg/L; DOC: 0.53–2.59 mg/L); mesotrophic waters (Funil Reservoir, chl-*a*: 4.92–52.78 μg/L; PC: 9.16–35.95 μg/L; TSS: 4.50–9.50 mg/L; DOC: 0.91–6.30 mg/L); and hypereutrophic waters (Catfish Ponds, chl-*a*: 59.40–1376.60 μg/L; PC: 68.13–857.08 μg/L).

spectral shape without a pronounced phytoplankton absorption feature typically observed between 665 and 685 nm. Spectral features such as low reflectance in blue and scattering in green are representative of waters with low chl-*a* concentration. The R_{rs} spectrum for the mesotrophic Funil Reservoir showed the lowest values in the blue wavelengths mainly due to a combined absorption by CDOM and chl-*a*. The trough around 625 nm is primarily associated with PC absorption (Schalles and Yacobi, 2000; Mishra et al., 2009; Mishra and Mishra, 2014). A pronounced trough at 675 nm caused by a strong chl-*a* absorption and when combined with the strong absorption by pure water in NIR, generates a peak near 700 nm. R_{rs} spectrum for the hyper-eutrophic Catfish Ponds with extremely high chl-*a* concentration showed the largest R_{rs} peak near 700 nm, mainly due to scattering by phytoplankton cells as well as two prominent troughs at 665 nm and around 620 nm caused by chl-*a* and PC absorption, respectively.

The variations in R_{rs} are related to the variations in IOPs, such as a_{phy}, a_{NAP}, and a_{CDOM} at each study site. The compositional variability of the IOPs can be visualized using ternary plots representing the absorption coefficients at three characteristic wavelengths, 440, 560, and 665 nm (Fig. 1.4).

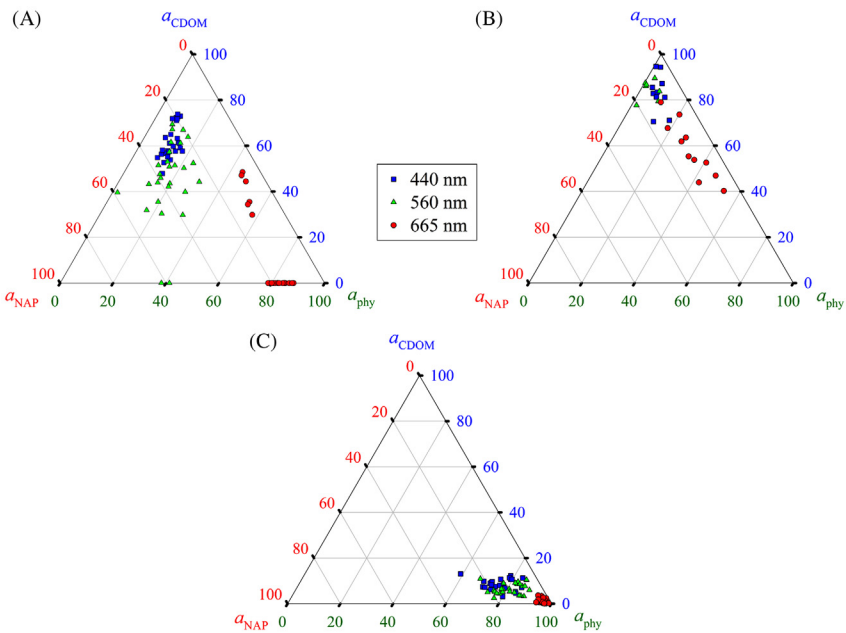

FIGURE 1.4 Ternary plots of absorption coefficients of CDOM, phytoplankton and NAP at three different wavelengths: 440 (square), 560 (triangle), and 665 nm (round). (A) oligotrophic Itumbiara Reservoir, Brazil; (B) eutrophic Funil Reservoir, Brazil; (C) hypereutrophic Catfish Ponds, USA.

Absorption coefficient at 440 nm is influenced by a combined absorption of CDOM, chl-*a* and tripton (Fig. 1.2). Absorption coefficient at 560 nm is usually governed by NAP absorption, and absorption coefficient at 665 nm is related to the absorption of chl-*a*. The ternary plot for Itumbiara Reservoir (Fig. 1.4A) showed a mix of CDOM and NAP dominance which can also be observed in its R_{rs} spectrum with only one prominent peak at around 550 nm (Fig. 1.3). The ternary plot for Funil Reservoir (Fig. 1.4B) showed that a_{CDOM} is the dominant IOP, which supported the very low value in the blue wavelength range observed in R_{rs} spectrum. The complete dominance of a_{phy} is clearly visible in the ternary plot for the hypereutrophic catfish ponds (Fig. 1.4C). These ternary plots exemplify the optical complexities of inland waters and how reflectance at certain spectral region (e.g., blue) is being influenced by multiple constituents. Because of that bio-optical models for inland waters are increasingly focused on red-NIR bands (e.g., Gurlin et al., 2011).

1.4 BIO-OPTICAL MODELS

The expression "bio-optical" was first used to describe the "state of ocean waters" (Smith and Baker, 1977). The term "state" is defined by Smith and Baker (1977) as the optical state of water, which is essentially controlled by the optical properties of the biological materials in the water column, mainly phytoplankton and its derivatives. However, the current use of the term "bio-optical" is often combined with models in remote sensing research. Bio-optical models are based on radiometric quantities or IOPs and AOPs, such as downwelling spectral solar and sky radiation and the absorption and scattering properties of constituents in the water column. Studies by Cox and Munk (1954), Petzold (1972), Jerlov (1968, 1976), Preisendorfer (1976), among numerous others, established the main theory of hydrologic optics (currently known as ocean optics) before or around the launch of one of the first Earth Observing Satellites, the Earth Resources Technology Satellites 1 (ERTS-1), in 1972. Subsequently, transformative research was conducted by Gordon et al. (1975) who developed the first bio-optical model. They used Monte Carlo simulation of the radiative transfer equations to develop relationship between AOPs and IOPs for oceanic waters. Since then, numerous other bio-optical models have been published for oceanic, coastal, and inland waters. Applications of these bio-optical models to inland waters have recently been highlighted by several studies. Although there is a rapid increase of studies on bio-optical modeling, there is a lack of consistency in terminology and classification of types of bio-optical models (Ogashawara, 2015).

Bio-optical models can be defined in two ways. The first definition refers to the various ways of describing the "bio-optical state" of the aquatic system (Morel, 2001). It means that the optical properties are a function of the

biological and geomorphological activities in the water body. Therefore, bio-optical models are often aimed at deriving information about the biological and physical processes in the water body by establishing relationships between radiometric measurements and optically active constituents. According to Morel (2001), these models are usually classified as empirical and descriptive based on statistical relationships between radiometric quantities. The second definition for bio-optical models refers to the use of the radiative transfer theory to derive optical properties of constituents in the water column (Mobley, 2001). These bio-optical models are based on the quantification of IOPs, which can be used to derive the composition of constituents through a ratio of their absorption coefficients (a) and specific absorption coefficients (a^*), and backscattering coefficients (b_b) and specific backscattering coefficients ($b_b{}^*$). These bio-optical models are usually referred to as analytical models.

Bio-optical models have been used to monitor the inland water quality, mainly estimating concentrations of chl-a, or TSS as indicators of the trophic or turbidity status of the water body, respectively. Bio-optical models have also been used to quantify biogeochemical fluxes and the underlying environmental forcing (Kutser et al., 2005b, 2009, Giardino et al., 2010). These models combined with multiplatform observations (in situ, airborne, and space-borne) can be extremely useful in understanding the feedback between the water body and surrounding landscape.

1.4.1 Classification of Bio-optical Models

Different terms have been used to classify bio-optical models according to their formulation and goals (Odermatt et al., 2012) due to a lack of consistency in generally agreed terminology. Based on the formulation and final goals of the bio-optical models found in the literature, models may be classified into five broad categories as empirical, semi-empirical, semi-analytical, quasi-analytical, and analytical (Ogashawara, 2015).

Empirical and semi-empirical models are usually based on statistical relationships between in situ measurements of water constituents and radiometric data from satellite sensor or proximal remote sensing devices. The difference between empirical and semi-empirical models relies on the assumptions used during their development; empirical models focus only on the statistical estimators. The formulae used in empirical models are based on a combination of R_{rs} at different wavelengths, which will provide the best correlation between reflectance data and the concentration of optically active water constituents. These types of models typically use statistical techniques, such as neural networks, least squares, and stepwise regressions to extract the best relationship between R_{rs} and constituent concentrations. The selection of spectral bands does not follow any physical or optical principles of the IOPs or AOPs.

Semi-empirical models, on the contrary, are based on specific spectral features of absorption and scattering of the constituents governing reflectance (e.g., Morel and Gordon, 1980). An example of a physical assumption used in semi-empirical models is the R_{rs} peak near 700 nm commonly used to estimate chl-*a* concentration in inland and coastal waters (Gitelson, 1992, 2005; Gurlin et al., 2011; Mishra and Mishra, 2012). It forms at that spectral region because of minimal combined absorption by chlorophyll and water and, thus, scattering is mostly pronounced in the reflectance spectra. The magnitude of the peak increases and position shifts toward longer wavelength with increase of chl-*a* concentration (Gitelson, 1992). The physical principle behind the characteristics of the 700 nm peak forms the basis for band selection in semi-empirical models unlike pure statistical relationship in case of empirical models. The outputs of semi-empirical models are usually related to water constituents via statistical estimators.

Semi-analytical and quasi-analytical models rely on the inversion of the radiative transfer equations to establish relationships among AOPs and IOPs, which is computed through several analytical and empirical steps. Inverse models use AOPs, such as reflectance above or below water surface (R_{rs} or r_{rs}, respectively) to derive IOPs (Gordon et al., 1975, 1988):

$$r_{rs}(\lambda) = \frac{L_u(0^-, \lambda)}{E_d(0^-, \lambda)} = g_1\left(\frac{b_b(\lambda)}{a(\lambda) + b_b(\lambda)}\right) + g_2\left(\frac{b_b(\lambda)}{a(\lambda) + b_b(\lambda)}\right)^2 \tag{1.1}$$

where: $r_{rs}(\lambda)$ is the remote sensing reflectance just below water surface, $a(\lambda)$ is the total spectral absorption coefficient, $b_b(\lambda)$ is the total spectral backscattering coefficient, $L_u(0^-, \lambda)$ and $E_d(0^-, \lambda)$ are upwelling radiance and downwelling irradiance, respectively, g_1 and g_2 are geometrical factors.

The main difference between semi-analytical and quasi-analytical models is the process used to estimate $a(\lambda)$ and $b_b(\lambda)$. In semi-analytical models, the estimation of $a(\lambda)$ is computed by the sum of a_{phy}, a_{NAP} and a_{CDOM}. To derive $a(\lambda)$ in quasi-analytical models, knowledge about other absorption coefficients is not necessary since it estimates $a(\lambda)$ directly from R_{rs} and the other absorptions coefficients are computed from the spectral decomposition of the estimated $a(\lambda)$ (Lee et al., 2002). For the $b_b(\lambda)$ estimation, semi-analytical models usually compute it as the sum of the backscattering coefficients for each water constituent except CDOM. In case of quasi-analytical models, $b_b(\lambda)$ is typically computed based on the widely used expression (Gordon and Morel, 1983):

$$b_b(\lambda) = b_{b,w}(\lambda) + b_{b,p}(\lambda_0)\left(\frac{\lambda_0}{\lambda}\right)^{\eta} \tag{1.2}$$

where λ_0 is the target wavelength, $b_{b,p}$ is backscattering coefficients of suspended particles and η is known as Angström exponent and related to the particle size distribution (see Chapter 2 for detail). The outputs from semi-analytical and quasi-analytical models estimated IOPs are validated using IOPs derived from water samples via analytical methods. A purely analytical model is based only on the physical properties of constituents, for example the one proposed by Bricaud et al. (1995) for the estimation of chl-*a* concentration by using the ratio of a_{phy} and the specific absorption coefficient of phytoplankton (a_{phy}^*) (Table 1.2).

Table 1.2 presents examples of the five types of bio-optical models used to estimate chl-*a* in inland waters from remote sensing data. Chl-*a* is shown as an example since it is one of the most widely studied water constituent in remote sensing. The first example is an empirical model proposed by Allan et al. (2015) who used an average reflectance in green and red spectral bands of Landsat5-TM to establish relationship between band ratio and chl-*a* concentration. The two-band (Gitelson, 1992) and three-band (Dall'Olmo and Gitelson 2005; Gitelson et al., 2003) semi-empirical models (not shown in Table 1.2) used reflectance in red and NIR spectral regions and have been widely applied to predict chl-*a* in inland waters. Similarly, Mishra and Mishra (2012) proposed a semi-empirical model, normalized difference chlorophyll index (NDCI), based on the difference between reflectance at 665 nm (MEdium Resolution Imaging Spectrometer, MERIS band 7) and 709 nm (MERIS band 9). Semi-analytical model proposed by Vos et al. (2003) is based on the spectral bands of Sea-viewing Wide Field-of-view Sensor (SeaWiFS). The model estimates $a_{phy}(670)$ by establishing relationship between several parameters (see Table 1.2). This model is classified as semi-analytical since $a(\lambda)$ is not required to estimate $a_{phy}(670)$. A quasi-analytical model reparametrized by Li et al. (2013) estimated the total absorption without the water absorption ($a_{t\text{-}w}$) from a relationship between R_{rs}, b_b, and a_w at 709 nm, $b_b(\lambda)$, and $a_w(\lambda)$. The model assumed that at 665 nm the total absorption is entirely caused by phytoplankton, and therefore, $a_{t\text{-}w}$ can be used to estimate chl-*a* concentration.

1.4.2 Performance of Bio-optical Models

Several studies have been published in recent years comparing the performance of existing semi-empirical bio-optical models, mainly for the estimation of chl-*a* concentration in inland waters. Gurlin et al. (2011) compared the performance of two-band (Gitelson, 1992) and three-band NIR-red models (Dall'Olmo et al., 2003; Dall'Olmo and Gitelson, 2005) using data from several productive lakes in Nebraska at MERIS spectral channels (Moses

TABLE 1.2 Examples of the Five Types of Bio-Optical Models used for chl-*a* Estimation

Model type	Reference	Sensor	Model structure
Empirical	Allan et al. (2015)	Landsat/TM	$Chl-a \cong \left(865.17 \bullet \left(\frac{B_{2+}B_3}{2}\right)^2\right) + \left(19.8 \bullet \left(\frac{B_{2+}B_3}{2}\right)\right) + 0.24$
Semi-empirical	Mishra and Mishra (2012)	MERIS	$Chl-a \propto \frac{R_{rs}(B_9) - R_{rs}(B_7)}{R_{rs}(B_9) + R_{rs}(B_7)}$
Semi-analytical	Vos et al. (2003)	SeaWiFS	$a_{phy}(670) = \left(\frac{fb_b(670)}{R_{rs}(670)}\right) - (b_b(670) + g_{440}\overline{a}_{CDOM}(670) + a_w(670) + a^*_{TSM}(670)C_{TSM})$
Quasi-analytical	Li et al. (2013)	Ocean Optics in situ sensor (USB-4000)	$a_{t-w}(\lambda) = \frac{R_{rs}(709)b_b(\lambda)[a_w(709) + b_b(709)]}{R_{rs}(\lambda)b_b(709)} - b_b(\lambda) - a_w(\lambda)$
Analytical	Bricaud et al. (1995)	Spectrophotometer	From inversion of a R_{rs} model

Note: There are numerous examples exist in the literature under each category.

et al., 2009a,b). The study showed that the two-band model was more accurate in estimating chl-*a* than the three-band model. Augusto-Silva et al. (2014) compared the performance of two- and three-band NIR-red models and NDCI at close range in an inland tropical reservoir and found that NDCI was the most accurate among the three models. Beck et al. (2016) compared 12 bio-optical models used for the estimation of chl-*a* concentrations in Harsha Lake, OH, USA by simulating reflectance at spectral bands of different sensors. The authors concluded that NDCI is the most widely applicable model and performs well for most of the sensors typically used in remote sensing for inland waters including MERIS, WorldView-2, MSI Sentinel-2, and OLCI Sentinel-3.

Odermatt et al. (2012) provided an overview of different semi-empirical and empirical bio-optical models for estimating water constituents using satellite data. The study evaluated different satellite sensors, such as Sea-Viewing Wide Field-of-View Sensor (SeaWiFS), Moderate Resolution Imaging Spectroradiometer (MODIS), MEdium Resolution Imaging Spectrometer (MERIS), Landsat, and Hyperspectral Imager for the Coastal Ocean (HICO) in order to compare the bio-optical models for chl-*a*, TSM and CDOM estimation (Figs. 1.5–1.7).

The Ocean Color (OC) series of models (O'Reilly et al., 2000) were able to estimate accurately the chl-*a* concentration in optically complex waters only for chl-*a* below 10 mg/m^3 (Fig. 1.5). For higher concentrations (10–100 mg/m^3), red-NIR based empirical and semi-empirical models were able to accurately estimate the chl-*a* concentration. More detailed insight into bio-optical modeling of chl-*a* (phytoplankton) and sun-induced chl-*a* fluorescence is provided in Chapter 6 and Chapter 7, respectively.

Fig. 1.6 shows a list of bio-optical models developed between 2006 and 2011 for TSM estimation. Although the study showed that different types of bio-optical models could be used to retrieve TSM, still there is a strong sensitivity of the models towards the concentration range at which these models perform accurately. None of the TSM models tested in this study performed accurately over a broad concentration range (0–1000 mg/m^3). The overestimation is because of the effects of chl-*a* and CDOM which often contribute to turbidity. A more detailed discussion about bio-optical models involving TSM (or TSS) estimation is presented in Chapter 5.

CDOM estimation models for SeaWiFS, MERIS, and MODIS imagery were also reviewed by Odermatt et al. (2012) (Fig. 1.7). They reported a similar bias in the performance of the models toward the CDOM range because CDOM absorption wavelength range (blue range) is usually affected by other water constituents. Chapter 4 of this book presents a complete review of remote sensing and bio-optical modeling of CDOM.

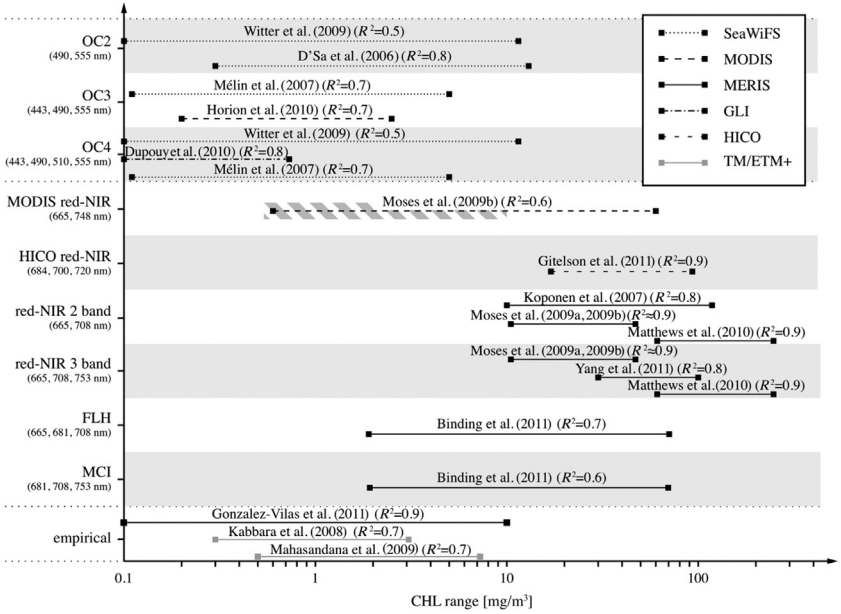

FIGURE 1.5 Performance summary of the semi-empirical and empirical models for chl-*a* estimation using various satellite sensors. *Source: Figure 1.1 from Odermatt et al. (2012).*

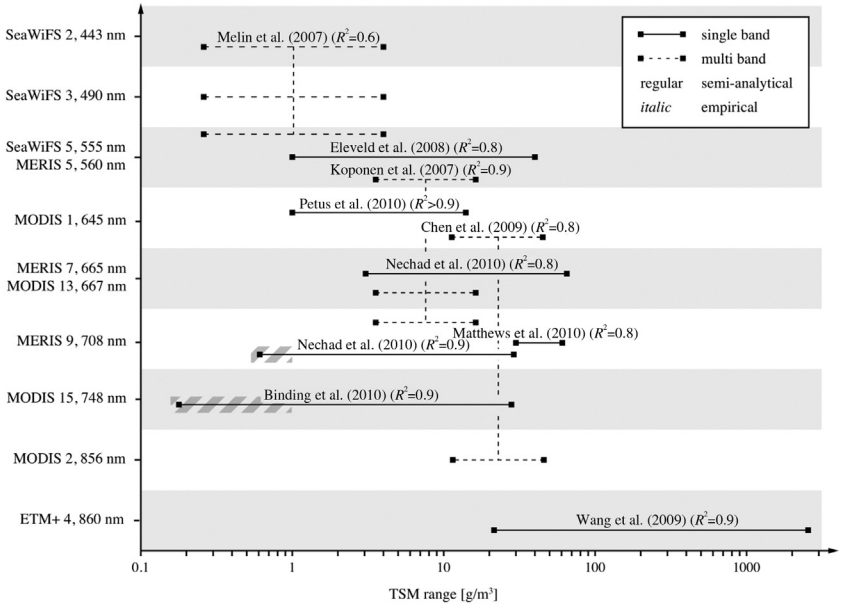

FIGURE 1.6 Performance summary of the semi-empirical and empirical models for TSM estimation using various satellite sensors. *Source: Figure 1.2 from Odermatt et al. (2012).*

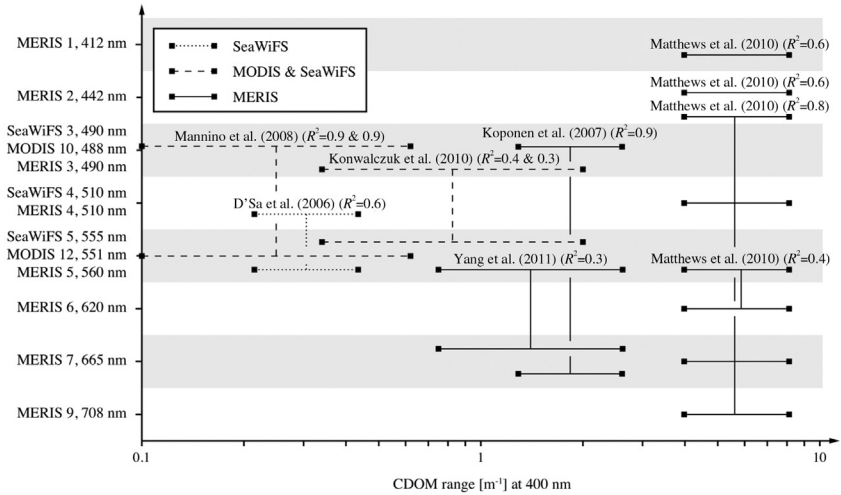

FIGURE 1.7 Performance summary of the semi-empirical and empirical models for CDOM estimation using various satellite sensors. *Source: Figure 1.3 from Odermatt et al. (2012).*

1.5 BOOK CONTENT

The book contains nine chapters covering key topics on remote sensing of inland waters. The topics were chosen based on a comprehensive review of remote sensing literature on inland waters. Remote sensing of inland waters is a complex problem because of the significant interaction between optically active constituents. Therefore, a fundamental understanding of the radiative transfer theory, optical properties of the water constituents, and existing bio-optical models is required to advance this field of research. This book covers all these topics in a comprehensive manner.

Chapter 2 provides an overview of radiative transfer theory describing the physical principles of interaction of light with constituents in the water column. For understanding the optical properties, such as IOPs and AOPs and bio-optical models, it is crucial to develop an insight to radiative transfer theory. The propagation of light through water and its absorption and scattering due to the interaction with constituents determines the radiant intensity or reflectance detected by a sensor deployed above or under water, be it in situ or airborne or space-borne. To decompose these composite reflectance spectra, one needs to understand the properties of the medium and the constituents in it. Chapter 2 breaks down the mathematical principles behind radiative transfer by IOPs, AOPs, constituents, geometric parameters, surface effects, and under water light field in a detail manner. It also provides a seamless transition to subsequent chapters, which deal with bio-optical modeling of optically active constituents.

Light received by an airborne or space borne remote sensor includes contributions due to its interactions with gaseous molecules and aerosol particles

in the atmosphere in addition to the light reflected directly from the water body. The effects of atmospheric interference need to be adequately corrected for prior to applying field-based bio-optical models to remotely sensed data. Atmospheric correction of remotely sensed data is more challenging for inland waters than for open ocean waters due to a number of factors. Chapter 3 lays out the challenges and provides a comprehensive review of several existing atmospheric correction algorithms for inland waters, with brief discussions of the basic assumptions underlying each algorithm.

Atmospheric correction chapter is followed by Chapters (4–8) dealing with bio-optical modeling of water constituents starting with CDOM. CDOM is the optically active part of carbon. In remote sensing, it can be used as a proxy of dissolved organic carbon in an aquatic system. CDOM increases radiative heating of water bodies, limits the amount of light available for primary production, and protects aquatic life from excessive solar radiation. Accurate modeling and quantification of CDOM is important in studying the role of inland waters in global carbon cycle. In addition to providing a broad overview of the importance of CDOM in inland waters, Chapter 4 discusses in detail the optical properties of CDOM and architecture of existing empirical and semi-analytical bio-optical models.

TSS, a proxy for sediment flux, contaminants, and pollutants, plays an important role in controlling primary productivity in inland waters. Fortunately, TSS is one of the frequently studied and accurately modeled water constituents in both inland and coastal waters. Chapter 5 reviews the optical properties of TSS, mainly absorption and backscattering properties in several subalpine lakes as case studies. It also discusses a list of models including empirical and semi-analytical those have been used successfully before. In addition to field-based models, Chapter 5 also presents scaled-up model case studies from rivers to deep lakes involving airborne data, and Landsat-8 and MERIS images.

Similar to TSS, chl-*a* is another frequently studied water constituent using remote sensing techniques. Chl-*a* concentration, a proxy for phytoplankton biomass and productivity, is one of the most important water quality parameters because of its sensitivity and quick response to environmental and landscape changes. Chapter 6 discusses the theoretical basis of principles for estimating chl-*a* using remote sensing measurements via the optical pathways of absorption, fluorescence, and scattering. It also discusses the challenges in estimating chl-*a* in inland waters such as interference from other constituents and models to address them.

Chapter 7 deals with a different aspect of chl-*a* estimation using the sun-induced chl-*a* fluorescence. This chapter is focused on analyzing the relationship between fluorescence and phytoplankton abundance, CDOM absorption, and TSS concentration using a four component bio-optical model implemented on simulated and field remote sensing data. The chapter also discusses the use and limitations of fluorescence line height algorithms for estimating chlorophyll from various satellite data including MERIS and MODIS, which

can be applicable also to Geostationary Ocean Color Imager and Sentinel-3's Ocean and Land Color Instrument. The detailed analysis of the models and remote sensing techniques presented in this chapter are useful for monitoring sun-induced chl-*a* fluorescence from water bodies over wide geographic regions and varied optical properties.

Although chl-*a* is commonly used for monitoring of algal blooms, remote estimation of cyanobacterial bloom is generally achieved through PC, a unique accessory pigment in cyanobacteria. Toxin producing cyanobacteria are a public health issue and frequent monitoring of these blooms may lead to targeted early warning systems, which would be extremely beneficial to human and animal health. Chapter 8 reviews the status of remote sensing of cyanobacteria using bio-optical models. It expands on the advantages and disadvantages of existing PC models and evaluates representative algorithms using a large field dataset. Discussions about the factors affecting the accuracy of the PC models will aid in developing scale-up techniques allowing their implementation on satellite data.

Submerged aquatic vegetation (SAV) or aquatic macrophytes grow in relatively clear water environments and provide suitable habitats for fish and zooplankton. They also influence the nutrient and energy cycling and limit phytoplankton growth. Developing remote sensing techniques to monitor their status and trend often leads to better water resource management. SAV can also act as a source of uncertainty for bio-optical models aimed at estimating water constituents by interfering with the remote sensing reflectance data. Therefore, isolating the SAV contribution in R_{rs} would lead to accurate estimation of the optically active water constituents. The final chapter of this book, Chapter 9 provides an overview of the current research on remote sensing of SAV. This chapter discuses several important topics, such as spectral properties of SAV, existing remote sensing models, application of airborne and space-borne data in mapping SAV biophysical properties, and need for regional assessment and global monitoring.

The content of this book summarizes the progress that has been made so far by remote sensing community worldwide on the broad topic of "remote sensing of inland waters." Although the bio-optical modeling of different water constituents is the main topic of this book, physical understanding of necessary theories to carry out bio-optical modeling, such as radiative transfer theory and atmospheric correction are also presented. Since it is a relatively new area of remote sensing research, there are several challenges that will not be easily solved, such as the development of robust and widely applicable radiative transfer models for inland waters. Nevertheless, the book discusses the theory and current state of the art in remote sensing of inland waters considering the availability of sensors with an adequate spatial, spectral, temporal, and radiometric resolution in future. The potential of these methods coupled with current and future satellite missions will enhance the opportunity to create an operational system or protocol for monitoring inland waters using remote sensing technologies.

REFERENCES

Allan, M.G., Hamilton, D.P., Hicks, B., Brabyn, L., 2015. Empirical and semi-analytical chlorophyll a models for multi-temporal monitoring of New Zealand lakes using Landsat. Environ. Monit. Assess. 187, 364. Available from: http://dx.doi.org/10.1007/s10661-015-4585-4.

Augusto-Silva, P.B., Ogashawara, I., Barbosa, C.C.F., de Carvalho, L.A.S., Jorge, D.S.F., Fornari, C.I., et al., 2014. Analysis of MERIS reflectance models for estimating chlorophyll-a concentration in a Brazilian Reservoir. Remote Sens. 6, 11689–117077.

Bastviken, D., Tranvik, L.J., Downing, J.A., Crill, P.M., Enrich-Prast, A., 2011. Freshwater methane emissions offset the continental carbon sink. Science 331, 50.

Bricaud, A., Babin, M., Morel, A., Claustre, H., 1995. Variability in chlorophyll-specific absorption coefficients of natural phytoplankton: analysis and parameterization. J. Geophys. Res. 100 (7), 13321–13332. Available from: http://dx.doi.org/10.1029/95JC00463.

Cox, C., Munk, W., 1954. Measurement of the roughness of the sea surface from photographs of the sun's glitter. J. Opt. Soc. Am. 44 (11), 838–850. Available from: http://dx.doi.org/10.1364/JOSA.44.000838.

Dall'Olmo, G., Gitelson, A.A., 2005. Effect of bio-optical parameter variability on the remote estimation of chlorophyll-a concentration in turbid productive waters: experimental results. Appl. Opt. 44 (3), 412–422. Available from: http://dx.doi.org/10.1364/AO.44.000412.

Dall'Olmo, G., Gitelson, A.A., Rundquist, D.C., 2003. Towards a unified approach for remote estimation of chlorophyll-a in both terrestrial vegetation and turbid productive waters. Geophys. Res. Lett. 30 (18), 1938. Available from: http://dx.doi.org/10.1029/2003GL018065.

Dekker, A.G., 1993. Detection of Optical Water Quality Parameters for Eutrophic Waters by High Resolution Remote Sensing. Ph.D. Thesis. Vrije Universiteit, Amsterdam, The Netherlands.

Duan, H., Ma, R., Xu, J., Zhang, Y., Zhang, B., 2010. Comparison of different semi-empirical models to estimate chlorophyll-a concentration in inland lake water. Environ. Monitor. Assess. 170, 231–244.

Giardino, C., Bresciani, M., Villa, P., Martinelli, A., 2010. Application of remote sensing in water resource management: the case study of Lake Trasimeno, Italy. Water Resour. Manag. 24, 3885–3899. Available from: http://dx.doi.org/10.1007/s11269-010-9639-3.

Gitelson, A., 1992. The peak near 700 nm on radiance spectra of algae and water: relationships of its magnitude and position with chlorophyll concentration. Int. J. Remote. Sens. 13, 3367–3373. Available from: http://dx.doi.org/10.1080/01431169208904125.

Gitelson, A.A., Gritz, U., Merzlyak, M.N., 2003. Relationships between leaf chlorophyll content and spectral reflectance and algorithms for non-destructive chlorophyll assessment in higher plant leaves. J. Plant. Physiol. 160 (3), 271–282.

Gitelson, A.A., Dall'Olmo, G., Moses, W., Rundquist, D.C., Barrow, T., Fisher, T.R., et al., 2008. A simple semi-analytical model for remote estimation of chlorophyll-a in turbid waters: Validation. Remote Sens. Environ. 112, 3582–3593. Available from: http://dx.doi.org/10.1016/j.rse.2008.04.015.

Gons, H.J., Auer, M.T., Effler, S.W., 2008. MERIS satellite chlorophyll mapping of oligotrophic and eutrophic waters in the Laurentian Great Lakes. Remote Sens. Environ. 112, 4098–4106. Available from: http://dx.doi.org/10.1016/j.rse.2007.06.029.

Gordon, H., Morel, A., 1983. Remote assessment of ocean color for interpretation of satellite visible imagery: a review. Lecture Notes on Coastal and Estuarine Studies. Springer Verlag, New York, NY, USA, p. 4.

Gordon, H.R., Brown, O.B., Jacobs, M.M., 1975. Computed relationships between the inherent and apparent optical properties of a flat homogeneous ocean. Appl. Opt. 14 (2), 417–427. Available from: http://dx.doi.org/10.1364/AO.14.000417.

Gordon, H.R., Brown, O.B., Evans, R.H., Brown, J.W., Smith, R.C., Baker, K.S., et al., 1988. A semianalytic radiance model of ocean color. J. Geophys. Res. 93 (D9), 10909–10924.

Gurlin, D., 2012. Near infrared-red models for the remote estimation of chlorophyll-α concentration in optically complex turbid productive waters: From in situ measurements to aerial imagery [doctoral dissertation]. Univ. of Nebraska-Lincoln.

Gurlin, D., Gitelson, A.A., Moses, W.J., 2011. Remote estimation of chl-a concentration in turbid productive waters—return to a simple two-band NIR-red model? Remote Sens. Environ. 115, 3479–3490. Available from: http://dx.doi.org/10.1016/j.rse.2011.08.011.

Hadjimitsis, D.G., Clayton, C., 2009. Assessment of temporal variations of water quality in inland water bodies using atmospheric corrected satellite remotely sensed image data. Environ. Monit. Assess. 159, 281–292.

Huang, C., Shi, K., Yang, H., Li, Y., Zhu, A., Sun, D., et al., 2015. Satellite observation of hourly dynamic characteristics of algae with Geostationary Ocean Color Imager (GOCI) data in Lake Taihu. Remote Sens. Environ. 159, 278–287. Available from: http://dx.doi.org/10.1016/j.rse.2014.12.016.

Jerlov, N.G., 1968. Optical oceanography, Elsevier Oceanographic Series, v. 5. Elsevier, Amsterdam, the Netherlands.

Jerlov, N.G., 1976. Marine optics, Elsevier Oceanographic Series, v. 14. Elsevier, Amsterdam, the Netherlands.

Kortum, G., 1969. Reflectance Spectroscopy. Principles, Methods, Applications. Springler-Verlag, New York Inc.

Kubelka, P., Munk, F., 1931. An article on optics of paint layers. Zeitschr. Fur techn. Physik 12, 593–601.

Kutser, T., Pierson, D.C., Tranvik, L., Reinart, A., Sobek, S., Kallio, K., 2005a. Using satellite remote sensing to estimate the colored dissolved organic matter absorption coefficient in lakes. Ecosystems 8, 709–720. Available from: http://dx.doi.org/10.1007/s10021-003-0148-6.

Kutser, T., Pierson, D., Kallio, K., Reinart, A., Sobek, S., 2005b. Mapping lake CDOM by satellite remote sensing. Remote Sens. Environ. 94, 535–540. Available from: http://dx.doi.org/10.1016/j.rse.2004.11.009.

Kutser, T., Paavel, B., Metsamaa, L., Vahtmae, E., 2009. Mapping coloured dissolved organic matter concentration in coastal waters. Int. J. Remote. Sens. 30, 5843–5849. Available from: http://dx.doi.org/10.1080/01431160902744837.

Kutser, T., Alikas, K., Kothawala, D.N., Köhler, S.J., 2015. Impact of iron associated to organic matter on remote sensing estimates of lake carbon content. Remote Sens. Environ. 156, 109–116. Available from: http://dx.doi.org/10.1016/j.rse.2014.10.002.

Le, C., Li, Y., Zha, Y., Sun, D., Huang, C., Lu, H., 2009. A four-band semi-analytical model for estimating chlorophyll a in highly turbid lakes: The case of Taihu Lake, China. Remote Sens. Environ. 113, 1175–1182. Available from: http://dx.doi.org/10.1016/j.rse.2009.02.005.

Lee, Z., Carder, K.L., Arnone, R.A., 2002. Deriving inherent optical properties from water color: a multiband quasi-analytical model for optically deep waters. Appl. Opt. 41 (27), 5755–5772. Available from: http://dx.doi.org/10.1364/AO.41.005755.

Li, L., Li, L., Song, K., Li, Y., Tedesco, L.P., Shi, K., et al., 2013. An inversion model for deriving inherent optical properties of inland waters: establishment, validation and application. Remote Sens. Environ. 135, 150–166. Available from: http://dx.doi.org/10.1016/j.rse.2013.03.031.

Matthews, M.W., Bernard, S., 2013. Characterizing the absorption properties for remote sensing of three small optically-diverse South African reservoirs. Remote Sens. 5, 4370–4404. Available from: http://dx.doi.org/10.3390/rs5094370.

Millennium Ecosystem Assessment (MEA), 2005. Ecosystems and Human Well-Being: Synthesis. Island Press, Washington, DC.

Mishra, S., Mishra, D.R., 2012. Normalized difference chlorophyll index: a novel model for remote estimation of chlorophyll-a concentration in turbid productive waters. Remote Sens. Environ. 117, 394–406. Available from: http://dx.doi.org/10.1016/j.rse.2011.10.016.

Mishra, S., Mishra, D.R., 2014. A novel remote sensing algorithm to quantify phycocyanin in cyanobacterial algal blooms. Environ. Res. Lett. 9, 114003. Available from: http://dx.doi.org/10.1088/1748-9326/9/11/114003.

Mishra, S., Mishra, D.R., Schluchter, W., 2009. A novel model for predicting phycocyanin concentrations in cyanobacteria: a proximal hyperspectral remote sensing approach. Remote Sensing 1 (4), 758–775. Available from: http://dx.doi.org/10.3390/rs1040758.

Mishra, S., Mishra, D.R., Lee, Z., Tucker, C.S., 2013. Quantifying cyanobacterial phycocyanin concentration in turbid productive waters: a quasi-analytical approach. Remote Sens. Environ. 133, 141–151. Available from: http://dx.doi.org/10.1016/j.rse.2013.02.004.

Mishra, S., Mishra, D.R., Lee, Z., 2014. Bio-optical inversion in highly turbid and cyanobacteria dominated waters. IEEE. Trans. Geosci. Remote. Sens. 52, 375–388. Available from: http://dx.doi.org/10.1109/TGRS.2013.2240462.

Mobley, C.D., 2001. Radiative transfer in the ocean. In: Steele, J.H. (Ed.), Encyclopedia of Ocean Sciences. Academic Press Elsevier, London, UK, pp. 2321–2330.

Mobley, C.D., Stramski, D., Bissett, W.P., Boss, E., 2004. Optical modeling of ocean waters: Is the Case 1-Case 2 classification still useful? Oceanography 17 (2), 60–67.

Morel, A., 2001. Bio-optical models. In: Steele, J.H. (Ed.), Encyclopedia of Ocean Sciences. Academic Press Elsevier, London, UK, pp. 317–326.

Morel, A., Gordon, H.R., 1980. Report of the working group on water color. Bound.-Layer Meteor. 18 (4), 343–355.

Morel, A., Prieur, L., 1977. Analysis of variation in ocean colour. Limnol. Oceanogr. 22, 709–722. Available from: http://dx.doi.org/10.4319/lo.1977.22.4.0709.

Moses, W.J., Gitelson, A.A., Berdnikov, S., Povazhnyy, V., 2009a. Estimation of chlorophyll-a concentration in case II waters using MODIS and MERIS data—successes and challenges. Environ. Res. Lett. 4/4, 045005. Available from: http://dx.doi.org/10.1088/1748-9326/4/4/045005.

Moses, W.J., Gitelson, A.A., Berdnikov, S., Povazhnyy, V., 2009b. Satellite estimation of chlorophyll-a concentration using the red and NIR bands of MERIS—the Azov Sea case study. IEEE Geosci. and Rem. Sens. Lett. 6 (4), 845–849.

National Research Council (NRC), 2002. The Drama of the Commons. National Academy Press, Washington, DC, USA.

O'Reilly, J.E., Maritorena, S., O'Brien, M.C., Siegel, D.A., Toole, D., Menzies, D., et al., 2000. SeaWiFS Postlaunch Calibration and Validation Analyses, Part 3, Volume 11. National Aeronautics and Space Administration, Washington, DC, USA.

Odermatt, D., Gitelson, A., Brando, V.E., Schaepman, M., 2012. Review of constituent retrieval in optically deep and complex waters from satellite imagery. Remote Sens. Environ. 118, 116–126. Available from: http://dx.doi.org/10.1016/j.rse.2011.11.013.

Ogashawara, I., 2015. Terminology and classification of bio-optical models. Remote Sens. Lett. 6 (8), 613–617. Available from: http://dx.doi.org/10.1080/2150704X.2015.1066523.

Ostrom, E., Stern, P.C., Dietz, T., 2003. Water rights in the commons. Water Resources IMPACT 5 (2), 9–12.

Peng, F., Effler, S.W., 2013. Spectral absorption properties of mineral particles in western Lake Erie: insights from individual particle analysis. Limnol. Oceanogr. 55 (5), 1775–1789. Available from: http://dx.doi.org/10.4319/lo.2013.58.5.1775.

Petzold, T.J., 1972. Volume Scattering Functions for Selected Ocean Waters (Ref. 72-28). Scripps Institute of Oceanography, University of California, San Diego, CA, USA.

Preisendorfer, R.W., 1976. Hydrologic Optics, Vol. II. Foundations. U.S. Dept. of Commerce, Washington, D.C., USA.

Schalles, J.F., Yacobi, Y.Z., 2000. Remote detection and seasonal patterns of phycocyanin, carotenoid, and chlorophyll pigments in eutrophic waters. Archi. Hydrobiol. 55, 153–168.

Smith, R.C., Baker, K.S., 1977. The Bio-Optical State if Ocean Waters and Remote Sensing. Scripps Institution of Oceanography, University of California, San Diego, CA, USA.

Simis, S.G.H., Peters, S.W.M., Gons, H.J., 2005. Remote sensing of the cyanobacterial pigment phycocyanin in turbid inland water. Limnol. Oceanogr. 50 (1), 237–245. Available from: http://dx.doi.org/10.4319/lo.2005.50.1.0237.

Song, K., Li, L., Tedesco, L., Clercin, N., Li, L., Shi, K., 2014. Spectral characterization of colored dissolved organic matter for productive inland waters and its source analysis. Chin. Geogra. Sci. 25 (3), 295–308. Available from: http://dx.doi.org/10.1007/s11769-014-0690-5.

Verpoorter, C., Kutser, T., Seekell, D.A., Tranvik, L.J., 2014. A global inventory of lakes based on high-resolution satellite imagery. Geophys. Res. Lett. 41, 6396–6402. Available from: http://dx.doi.org/10.1002/2014GL060641.

Vos, R.J., Hakvoort, J.H.M., Jordans, R.W.J., Ibelings, B.W., 2003. Multiplatform optical monitoring of eutrophication in temporally and spatially variable lakes. Sci. Total. Environ. 312, 221–243, http://dx.doi.org/10.1016/S0048-9697(03)00225-0.

Yacobi, Y., Gitelson, A., Mayo, M., 1995. Remote sensing of chlorophyll in Lake Kinneret using high spectral resolution radiometer and Landsat Thematic Mapper: spectral features of reflectance and algorithm development. J. Plankton Res. 17 (11), 1–19.